Chemical Engineering Journal 481 (2024) 148615

Contents lists available at ScienceDirect

Chemical Engineering Journal

journal homepage: www.elsevier.com/locate/cej

Easy fabrication method of Li_4SiO_4-K_2CO_3 based pellets for CO_2 capture at high temperature

Damiano Rossi [a,*], Irene Anguillesi [a], Umberto Desideri [b], Maurizia Seggiani [a]

[a] Department of Civil and Industrial Engineering, University of Pisa, Largo Lucio Lazzarino, 56122 Pisa, Italy
[b] Department of Engineering for Energy, Systems, Territory and Constructions, University of Pisa, Via Carlo Francesco Gabba 22, 56122 Pisa, Italy

ARTICLE INFO

Keywords:
CO_2 capture
Lithium orthosilicate
Potassium carbonate
Sorbents
Pellets
Eutectic powders
Polyalphaolefin

ABSTRACT

This study focuses on a novel fabrication method of K_2CO_3-Li_4SiO_4 based sorbents for CO_2 capture from hot flue gas of gas turbines. The developed pellets were produced by sintering K_2CO_3-Li_4SiO_4 powders at 550 °C using viscous polyalphaolefins as pore formers. This mild calcination temperature was selected as the optimal condition for the development of a suitable porosity preventing powder degradation which typically occurs at higher temperatures. The sorption/desorption performance was tested by thermogravimetric analysis conducted at 580 °C under 0.04 atm of CO_2 and 620 °C under 1 atm of N_2, respectively. Results showed that the use of 20 wt% K_2CO_3 represents the optimal content to achieve a stable formation of molten eutectic K_2CO_3-Li_2CO_3 mixture during CO_2 chemisorption, while avoiding K_2CO_3 crystals phase segregation during multiple sorption cycles. In addition, the use of 30 wt% olefin allowed the development of resistant and porous pellets of tuneable dimension and shape with a stable sorption capacity up to 130 mg_{CO2}/g obtained over 25 multiple cycles of 30 min each. The present research lays the groundwork for the adoption of a novel pelletizing technique to produce innovative sorbents with enhanced CO_2 capture and cycling capabilities, manufactured via a simple and more sustainable approach.

1. Introduction

Around 40 % of all anthropogenic CO_2 emissions responsible for global warming are emitted by power plants that burn fossil fuels such as coal, oil, natural gas, and biomass [1]. Over the past decades, several strategies have been employed to reduce CO_2 greenhouse gases and mitigate the severity of future climate change. Any technology for CO_2 capture aims to create concentrated CO_2 streams that can be easily transported or stored in geological formations (depleted oil and gas fields, salty formations, and non-extractable coal seams) [2]. Post-combustion treatments of hot flue gases from power plants such as wet absorption, dry adsorption, membrane, and cryogenic separation are the most popular methods used for CO_2 capture. Among them, wet absorption using amine solutions is the only method that has reached the required technology readiness level to be adopted on a large commercial scale [3]. Unfortunately, this technique involves a significant energy penalty due to the high energy requirement for solvent regeneration. Moreover, high absorption–desorption columns are necessary to reach high CO_2 abatement efficiency (>90 %), hence raising capital costs. Lastly, solvent degradation in the presence of oxygen-rich flue gases and high corrosion rate require elevated maintenance costs and pose relevant process challenges [3,4].

In recent years, solid sorbents such as those based on CaO, ceramics [5], zeolites [6], active carbons, and molecular sieves [7] have attracted the greatest interest in post-combustion CO_2 capture at low partial pressure. This is due to their intrinsic benefit of application in a wider temperature range, from ambient temperature up to 700 °C, less waste production during sorbent regeneration, and easy exhausted sorbent disposal. Among these solid sorbents, those based on lithium orthosilicate (Li_4SiO_4) are one of the most promising solutions for CO_2 capture at high temperatures and relatively high concentrations which is drawing worldwide research interest [8,9]. Li_4SiO_4 shows high CO_2 sorption capacity (up to 367 mg/g), good cyclic stability, and relatively low regeneration temperatures according to the following sorption/desorption reversible reaction:

$$Li_4SiO_4\,(s) + CO_2\,(g) \leftrightarrow Li_2CO_3\,(s) + Li_2SiO_3\,(s) \quad (1)$$

CO_2 sorption process on Li_4SiO_4 sorbent is governed by two stages: a first fast-chemisorption stage during which carbonation products accumulate

* Corresponding author.
E-mail address: damiano.rossi@unipi.it (D. Rossi).

https://doi.org/10.1016/j.cej.2024.148615
Received 1 November 2023; Received in revised form 21 December 2023; Accepted 5 January 2024
Available online 6 January 2024
1385-8947/© 2024 The Authors. Published by Elsevier B.V. This is an open access article under the CC BY license (http://creativecommons.org/licenses/by/4.0/).

on the particle surface forming single or double shell morphological configurations [10,11], followed by a second CO_2, Li^+, and O^{2-} slow-diffusion stage through the various product layers. CO_2 diffusion is usually regarded as the rate-limiting step due to its larger molecular diameter [12,13]. This limit becomes particularly important at low CO_2 partial pressures (<0.1 atm). For this reason, the performance improvement of Li_4SiO_4-based sorbents is mostly focused on the limitation of the CO_2 diffusion-controlled stage. Specifically, these enhancement approaches include granulation methods, optimization of new synthetic routes by means of more efficient silicon and lithium sources, transition metals doping, and alkali metal carbonates addition [9,14]. Most of the previous methods have successfully enhanced CO_2 sorption performance at different levels. In particular, the addition of alkali metal carbonates such as Na_2CO_3, $MgCO_3$, $CaCO_3$, and K_2CO_3 has shown the most promising results in improving the Li_4SiO_4 sorption capacity. This is due to the formation of molten eutectic carbonate mixtures with the Li_2CO_3 product at relatively high sorption temperatures (above 500 °C) which significantly decrease CO_2 diffusion resistance throughout the liquid eutectic layer. Among the various metal carbonates, K_2CO_3 has been particularly studied as adsorption promoter [15,16]. Kato et al. 2002 first demonstrated that 10 mol.% K_2CO_3 could improve CO_2 sorption capacity of modified lithium orthosilicate powders up to $\simeq$ 270 $mg_{CO2}/g_{sorbent}$ at 0.2 atm of CO_2 and 500 °C [17]. Then, extensive work on K_2CO_3 addition was carried out by Seggiani et al., 2011, 2013 showing that 30 wt% K_2CO_3 (respect to Li_4SiO_4) is the optimum value in terms of sorption capacity and good cyclic stability operating at 580 °C and 0.04 atm of CO_2 in absorption and 620 °C under 1 atm of N_2 in desorption [18,19]. Similar conditions were obtained by Zhang et al. 2014 and Zhou et al. 2017 who studied K_2CO_3-Li_4SiO_4 based powders under a humidified atmosphere and acidic conditions [20,21]. The presence of the molten eutectic layer was confirmed by Yang et al. 2016 via in situ XRD analysis coupled with differential scanning calorimetry [15]. The eutectic phase is composed by the mixture of two different phases, K_2CO_3 and Li_2CO_3, where the second carbonate is formed during the CO_2 capture process.

CO_2 capture studies reported in literature using K_2CO_3-Li_4SiO_4 based powders have been investigated and optimized under a plethora of different experimental conditions mainly using sorbent powders. However, the suitability of a specific sorbent should be assessed under more realistic parameters, such as actual temperature, atmosphere, gas flow rate, pressure, etc. In addition, more practical apparatus such as packed-column and fixed-bed reactors filled with solid pellets or monolithic structures are typically employed in industrial sorption processes. The use of solid and resistant pellets is a fundamental requirement in the design of optimal solid sorbents. In fact, fine powders cannot be used in continuous regenerable looping systems where they are elutriated out by the gas stream. Unfortunately, the literature on the development of lithium ceramics pellets has so far been scarce compared to the vast scientific production concerning lithium-based ceramic powders. The first study on Li_4SiO_4 pelletisation was carried out by Kato et al. 2004 who kneaded cylindrical Li_4SiO_4-Li_2ZrO_3 sorbents and found that the addition of 5 wt% Li_2ZrO_3 could stabilize the sorbent during cycling [22]. Essaki et al. 2005 evaluated the adsorption performance of Li_4SiO_4-K_2CO_3-Li_2ZrO_3 spherical pellets (5 mm) commercially available from Toshiba Ceramics Co. Ltd using a packed-bed reactor. In this case the fastest sorption-rate under 0.2 atm of CO_2 was reached at 500 °C, however, no information on the stability over long cycling was conducted [23,24]. To further improve sorbent cyclic stability layered graphite was introduced as pore former in K_2CO_3-Li_4SiO_4 based pellets obtained by mechanical press. However, pelleted graphite sorbents still exhibited lower sorption rates than the powders ones [25]. Spheronized pure Li_4SiO_4 pellets (from 2 to 4 mm) with high compression strength (2.84 MPa) and attrition resistance were produced by Yang et al. 2018 and Hu et al. 2019 using graphite and cellulose as pore formers, respectively. The pellets showed a good sorption capacities of about 150–220 $mg_{CO2}/g_{sorbent}$ over 50 cycles at 0.15 atm of CO_2 but still lower performance than original powders and significant sorption capacity loss over time [26,27]. Recently, polyethylene (20 wt%) has been investigated as pore former in the production of K_2CO_3-Li_4SiO_4 spheronized pellets with excellent compression and attrition resistance and sorption capacity up to 310 $mg_{CO2}/g_{sorbent}$ over 40 cycles [28]. Finally, a few studies have been proposed to simplify the overall production and pelletisation processes of lithium ceramics sorbents by means of novel single-step calcination methods [29], and sol–gel drip casting approach using cellulose and polyvinyl alcohol as pore former, respectively [30,31].

Unfortunately, most of the aforementioned pelletisation methods still involve complex calcination processes, multi-step techniques using solvents, binders, and pore former agents that are difficult to handle and mix with Li_4SiO_4-K_2CO_3 powders. Hence, high pressure mechanical pressing, moulding and spheronization techniques are often required to evenly disperse the various additives with the powders and shape the mixtures into semi-solid pastes that are finally calcinated. All these processes lead to material fragmentation, particle elutriation and sorbent waste. Furthermore, most of the Li_4SiO_4-based pellet development studies are conducted under unrealistic conditions using very high CO_2 concentrations that do not reproduce the CO_2 concentrations of exhaust hot gases for which Li_4SiO_4 pellets are designed.

To overcome these issues, the present work introduces an innovative and scalable single-step method of Li_4SiO_4 pellet fabrication. Li_4SiO_4 powders were produced by solid-state method using crystalline SiO_2 and Li_2CO_3 as precursors and then, K_2CO_3 was added at several amounts as activity promoter. In addition, commercially available polyalphaolefins were selected to form extrudable pastes that were modeled and then calcinated obtaining solid regenerable sorbents for the CO_2 capture from hot flue gas of gas turbines. Linear alpha olefin are employed due to their greater film thickness, no solubility with Li_4SiO_4 and K_2CO_3, high shear stability, low pour point, high viscosity index, no sulphur or nitrogen that act as CO_2 inhibitors in Li_4SiO_4 [32], and low degradation temperatures which allow the development of cavities and porosity within the pellet during calcination.

The sorption–desorption behaviour of the powders and developed pellets was tested in a thermal gravimetric analyser according to the optimized conditions found in previous articles [18,19,25,33]. The experimental data of CO_2 chemisorption were fitted to the Double Exponential Model (DEM) [14] to identify the rate-limiting step. X-ray diffraction (XRD), scanning electron microscopy (SEM), rheological measurements and nitrogen sorption BET tests were used to characterize the sorbents and understand the relationship between sorbent structure and CO_2 sorption properties as well as to detect morphological changes during multiple sorption/desorption cycles.

2. Experimental

2.1. Materials

Lithium carbonate Li_2CO_3 (1–5 μm) and crystalline quartz SiO_2 (1–5 μm), purchased from Sigma-Aldrich Co. Llc, were used as precursors of Li_4SiO_4. Potassium carbonate K_2CO_3 (10–20 μm), from Sigma-Aldrich Co Llc, was used as activity promoter. Polyalphaolefins Durasyn®168 (Y) and Durasyn®180 (I) purchased from Ineos Ltd were chosen as skeleton template as well as pore-forming material. These are 1-decene cross-linked olefins having a viscosity of 46 cSt (Y) and 1250 cSt (I), respectively, depending on the content of dimers, trimers, and tetramers. Polyacrylonitrile fibres (10–20 μm) (P) and dissolving pulp cellulose fibres (10–20 μm and α-cellulose 94 wt%) (D), provided by MAE SpA, were also used as porosity promoters.

2.2. Powders and pellet preparation

Li_4SiO_4 powders were synthesized from crystalline quartz SiO_2 and lithium carbonate Li_2CO_3 by solid-state method [18,19,25,33]. The two

compounds were initially mixed in the 2:1 (Li_2CO_3:SiO_2) molar ratio with an equal amount in weight of distilled water using an agate mortar and pestle. The aqueous slurry mixture was heated to 900 °C using a heating ramp of 1 °C/min and calcinated for 4 h. The resulting powders were ground by an electric agate mortar for 5 h and then sieved to obtain fine Li_4SiO_4 powders (<20 μm). K_2CO_3 was mixed to Li_4SiO_4 powders to produce powders at different K_2CO_3 concentrations used as reference samples. Li_4SiO_4 powders with 10, 20, and 30 wt% K_2CO_3 by total weight were named as K10, K20, and K30, respectively.

The best performing powder in terms of CO_2 sorption capacity was mixed with 30, 40, and 50 wt% (based on the total weight of powders) of polyalphaolefins Durasyn®168 (Y) and Durasyn®180 (I). To further improve pellet micro-porosity the resulting mixture was blended with 2 wt% (based on the total weight of powders) of polyacrylonitrile synthetic fibres and dissolving pulp cellulose fibres. Higher fibrous content (>2 wt%) hinders effective amalgamation, resulting in increased viscosity rendering the powder challenging to mould. Both olefins and fibres were manually mixed to the selected K_2CO_3-Li_4SiO_4 based powder by a mortar and pestle till obtaining a viscous paste which was then shaped to form the ceramic sorbents. Hence, pellets with different diameters (up to 15 mm) were produced by extruding the pastes with a glass syringes mounted on a KDS Legato™ 100 pump. Finally, the extruded pellets were calcinated in a muffle at 1 atm and at 550 and 900 °C for 4 h (heating/cooling rate 1 °C/min) to remove the pore formers by combustion and obtain pellets with the porosity necessary for an effective absorption of CO_2 and, at the same time, maintaining adequate solidity.

2.3. Powders and pellet characterization

Powder X-Ray Diffraction (XRD) patterns of the synthesized Li_4SiO_4 powders were collected using a Bruker D2 Phaser diffractometer (Bruker Corporation, Billerica, MA, USA) operating at 30 kV and 10 mA in θ-θ scan mode with Ni-filtered CuKα radiation (λ = 1.54 Å) and equipped with a one-dimensional Lynxeye detector. The XRD patterns were recorded over 5–65 2θ range, using a step size of 0.03°, and a counting time 3 s/step. Phase identification was verified by comparison against the corresponding Joint Committee Powder Diffraction Standards (JCPDS).

Samples morphology was examined using a Quanta™ FEG 450 scanning electron microscope (SEM) equipped with EDS by FEI Quanta ESEM Instrument (Hillsboro, OR, USA). Prior to the analysis, the surfaces were sputtered with a thin gold layer using an Edwards Sputter Coater apparatus. In addition to SEM analysis, optical microscopy was carried out on the powders samples and pellets using a Leica S9i stereo microscope equipped with a CCD camera (Wetzlar, Germany).

Brunauer, Emmett and Teller (BET) surface area of sorbents (powders and pellets) was derived from nitrogen/helium sorption isotherms following ISO 9277:2022 using a Micromeritics® TriStar II Plus Surface Area and Porosity Analyzer (Norcross, US). Prior to BET analysis samples were degassed at 250 °C for 3 h under nitrogen.

To evaluate powders extrudability and deformability prior high temperature sintering, melt rheological measurements were conducted on the selected modified powder pastes at temperatures of 30 and 50 °C using an MCR 92 Rheometer manufactured by Anton Paar (Graz, Austria). The instrument is equipped with a plate-plate configuration with a diameter of 25 mm and a 1 mm gap. An amplitude sweep was conducted to determine the linear viscoelastic limit and establish the operational parameters. The strain applied was 0.2 %. Subsequent assessments were carried out through oscillatory frequency sweeps spanning from 0.05 to 100 Hz (equivalent to 0.314 to 628 rad/s). The complex viscosity η* was measured as functions of angular frequency ω.

2.4. CO_2 sorption/desorption tests

The CO_2 sorption/desorption performance of the developed powders and pellets were evaluated through thermogravimetric analysis (TGA Netzsch STA 2500 Regulus, Germany). About 15 mg of each sorbent (powder or pellet) were loaded in an alumina pan and preconditioned at 580 °C for 2 h in N_2 flow (150 ml/min) using a heating rate of 20 °C/min to ensure moisture removal till sample weight resulted stable. Then, consecutive adsorption/desorption cycles (up to 25) were carried out at 580 °C under 0.04 atm CO_2 (N_2 balance) flow rate (150 ml/min) and at 620 °C under N_2 flow rate (150 ml/min), respectively, using a heating rate of 20 °C/min. Two adsorption/desorption times (2 h and 30 min each) were used to assess sorbent performance and cyclic stability. In fact, the potential to regenerate the sorbent while maintaining its sorption efficiency through multiple sorption/desorption cycles greatly influences the overall operating expenses of the system as well as their industrial applicability.

The conversion of Li_4SiO_4 ($X_{Li4SiO4}$) and the total CO_2 sorption capacity (mg_{CO2}/g) were calculated to quantify and compare the performance of the sorbents as follows:

$$X_{Li4SiO4}(\%) = 100 \cdot \frac{\Delta w}{f_{Li4SiO4} \cdot r_s} \quad (2)$$

where Δw is the weight increase, attributable to the CO_2 absorbed, per starting sorbent weight, $f_{Li4SiO4}$ is the weight fraction of the Li_4SiO_4 in the sorbent, and r_s is the stoichiometric uptake of CO_2 by Li_4SiO_4 which is 367 mg CO_2 per gram of Li_4SiO_4.

Double exponential model was used to fit the sorption data of the modified powders and pellets and quantify the relevance of the CO_2 chemical reaction over diffusion [24,25,34]:

$$y = Ae^{-K_1 t} + Be^{-K_2 t} + C \quad (3)$$

In this equation, y represents the weight increase percentage of the sorbent associated with the CO_2 adsorbed, while K_1 (s^{-1}) and K_2 (s^{-1}) are the kinetic parameters associated with the CO_2 superficial reaction and diffusional-controlled processes, respectively. The pre-exponential factors A and B indicate the respective controlling intervals for the CO_2 capture process: A relates to the chemical reaction, while B relates to diffusion. The C parameter is the y-intercept.

3. Results and discussion

3.1. Modified powders characterization

The XRD pattern of the synthesized Li_4SiO_4 powder reported in Fig. 1 displays the distinctive peaks of monoclinic Li_4SiO_4 [35]. The diffraction pattern demonstrates the complete reaction between SiO_2 and Li_2CO_3

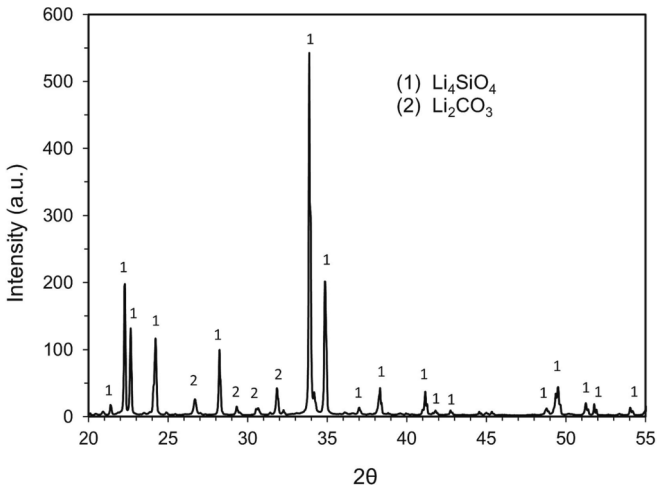

Fig. 1. XRD pattern of Li_4SiO_4 monoclinic powder synthesized by solid-state method [35].

precursors to Li_4SiO_4. The very minor peaks in the 25-35° range associated with Li_2CO_3 indicates the slight excess of Li_2CO_3 over SiO_2 and shows the practical difficulty of dosing the two precursors in the perfect stoichiometric 2:1 ratio. Furthermore, the slight presence of Li_2CO_3 and other impurities may also be attributed to an incomplete conversion of SiO_2, which subsequently carbonates, particularly at high temperatures in contact with air [33,35].

Fig. 2A-B shows the sorption–desorption curves of the K10, K20, and K30 powders. As expected, the eutectic formation significantly enhances the sorption performance of the powders compared to pure Li_4SiO_4: from $X_{Li4SiO4}$ of 5 % and about 6 mg_{CO2}/g for Li_4SiO_4 to $X_{Li4SiO4}$ of 90 % and about 250 mg_{CO2}/g for K30). In our case, the partial pressure is sufficiently low to replicate CO_2 capture from the hot flue gas of real gas turbines (0.04 atm). Consequently, under these conditions, as soon as a thin layer of Li_2CO_3 forms, the adsorption rate decays, rendering the inner Li_4SiO_4 almost unusable in a reasonable time. Pure Li_4SiO_4 has in fact a very limited cyclability with only one working cycle. These results are in accordance with other studies conducted in similar conditions [18,19]. The reason for the notably limited performance of pure Li_4SiO_4 in our tests may be attributed to the particularly fine particle sizes of the initial Li_4SiO_4 powders (1–20 μm). These sizes are smaller than the ones obtained in previous works, leading to higher particle-to-particle packing during cycling. This packing hinders CO_2 diffusion in the absence of a eutectic phase.

Among the powders K20 presents the best cycle stability across the eight cycles and the best sorption capacity. The lower values obtained by K10 are associated with a reduced molten eutectic mixture formation compared to K20 and K30, resulting in a minor enhancement of CO_2 diffusion and, therefore, minor Li_4SiO_4 conversion. Furthermore, with reference to the K_2CO_3-Li_2CO_3 binary system diagram of Fig. 3 [36], the determination of the $Li_2CO_3/(K_2CO_3 + Li_2CO_3)$ molar ratios *m* at end of the various cycles (assuming $X_{Li4SiO4} \simeq 0.9$, 0.8, and 0.5 % for K30, K20, and K10, respectively), shows an almost complete absorption/desorption permanence within the eutectic liquid phase for both K30 and K20 ($m = 0.7$ and 0.78, respectively). Unlike K10 ($m = 0.84$) which crosses the *right-liquidus curve* with consequent formation of the Li_2CO_3 solid phase s_3 which does not contribute to the CO_2 sorption process.

The previous findings are confirmed by the trends of the kinetic parameters K_1 and K_2 reported in Fig. 4A-B obtained by fitting the sorption curves of Fig. 2B with the double exponential model (Eq. (3). Results show that K_1 decreases, and K_2 increases with K_2CO_3 addition. This proves that reaction plays a marginal role over diffusion at high K_2CO_3 due to increased molten eutectic formation which enhances diffusion mechanism over reaction one. Generally, K_1 values are approximately one order of magnitude greater than K_2 values. This outcome is in agreement with previous research and suggests that the diffusion is the rate-determining step of CO_2 adsorption [25,37].

K30 presents an unstable behaviour with K_2 reaching a maximum plateau after three cycles. This material inertia might be caused by the large amount of K_2CO_3 present in the powder which requires a few cycles to compact forming a homogeneous molten layer. On the other hand, once the *m* ratio reaches the *left-liquidus curve*, K_2CO_3 crystals start forming and precipitating out of the liquid Li_2CO_3/K_2CO_3 mixture, resulting in a biphasic system. As desorption continues, the growing solid phase hinders the diffusion of CO_2 from the inner layers, leading to an anticipated decrease of the overall desorption rate [25].

Fig. 5 shows the SEM images of Li_4SiO_4 (Fig. 5A-B), K10 (Fig. 5C-D), K20 (Fig. 5E-F), and K30 (Fig. 5G-H) before and after eight sorption/desorption cycles. Pure Li_4SiO_4 (Fig. 5A) presents irregular particles and agglomerates in the 1–20 μm range. The addition of an increasing content of K_2CO_3 is visible in the form of larger particles (up to ≃ 50 μm) in K10 (Fig. 5C), K20 (Fig. 5E), and K30 (Fig. 5G) samples. The morphology of the powders changes significantly after eight cycles. Pure Li_4SiO_4 particles (Fig. 5B) result smooth and less irregular compared to the uncycled ones. This effect is likely caused by the consecutive carbonation/decarbonation processes, which level the external particle surfaces that remain largely disconnected from each other. The introduction of K_2CO_3 tends to agglomerate the original particles into smooth porous eutectic networks, developing 10–100 μm cavities responsible for the improved CO_2 diffusion sorption process [19,21]. In fact, the K10 powders subjected to cycles show more regular particles that are closely packed (Fig. 5D), and the increasing content of K_2CO_3 in K20 (Fig. 5F) leads to an interconnected structure created by the larger amount of molten eutectic phase bridging the gaps between particles, reshaping the morphology into a "spongy" type of network. The maximum K_2CO_3 content (K30) leads to the precipitation of carbonates as needles accumulated on the internal network cavities (Fig. 5H). The EDS conducted on these K30 needles (Fig. 7A) showed a potassium-rich phase compared to a lower concentration measured on K30 homogeneous surfaces (Fig. 7B). This result validates the K_2CO_3 segregation mechanism previously discussed in the K_2CO_3-Li_2CO_3 binary system diagram of Fig. 3, which is more relevant in the K30 sample exhibiting the highest K_2CO_3 content. The tendency of the eutectic phase to merge the particles into a continuous homogeneous network is evident when comparing the various powders after cycling. Pure Li_4SiO_4 does not develop a eutectic phase, thus the powders after cycles performed in TGA result desegregated, disperse, and friable as they were at the beginning (Fig. 6A). Conversely, cycled K_2CO_3-Li_4SiO_4, such as K20 and K30, form compact solid tablet structures due to the consecutive melting and solidification phases occurring during the absorption and desorption steps, respectively (Fig. 6B).

Considering the good sorption performance and the higher stability of K20 over K10 and K30, K20 was selected for the following pelletisation procedure using the various pore formers.

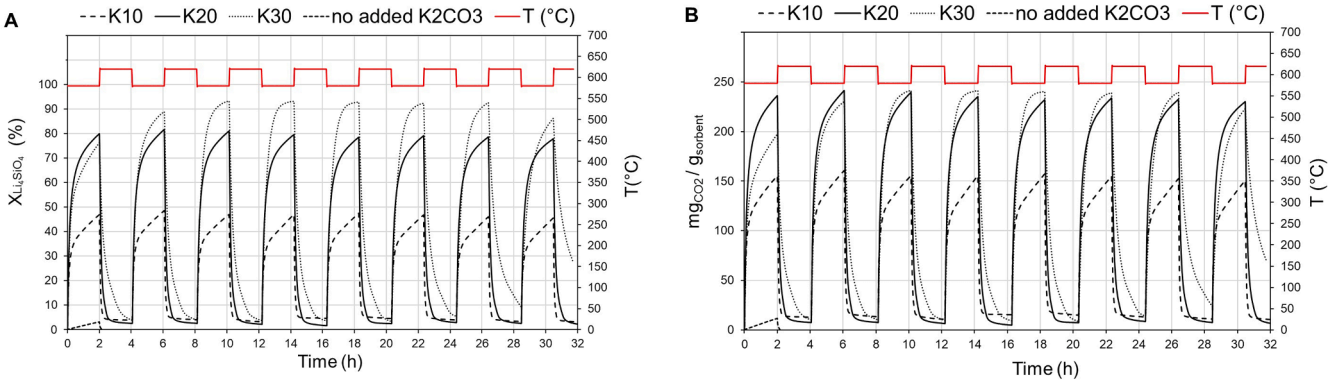

Fig. 2. Eight CO_2 sorption/desorption cycles in terms of conversion (**A**) and capacity (**B**) of Li_4SiO_4, K10, K20, and K30 powders under 0.04 atm CO_2 sorption at 580 °C (2 h) and 1 atm N_2 desorption at 620 °C (2 h).

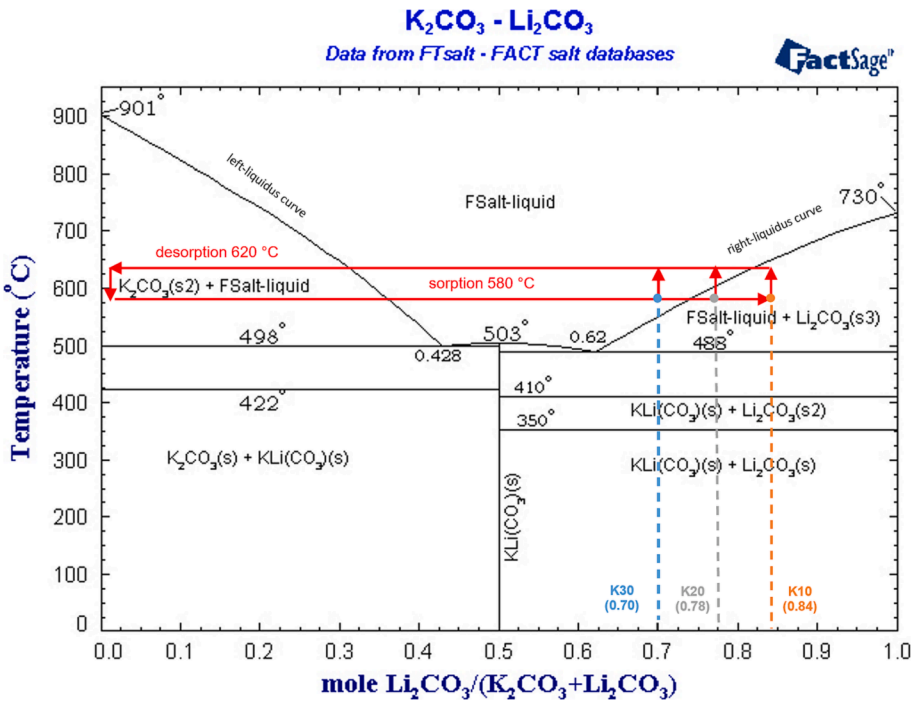

Fig. 3. Phase diagram of Li_2CO_3-K_2CO_3 system from FTsalt-FACT salt databases [36].

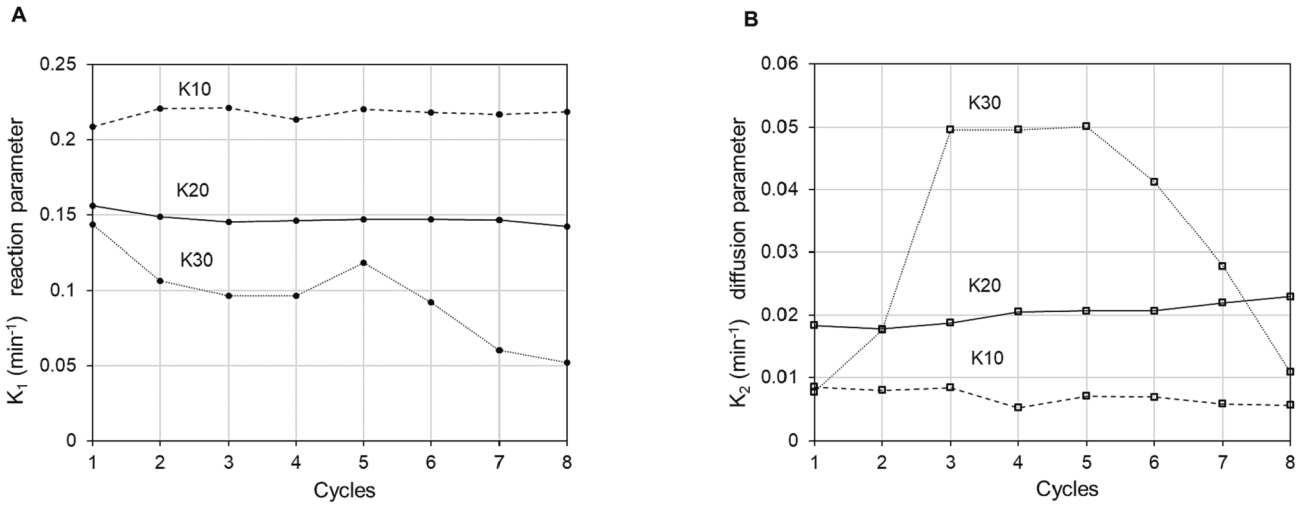

Fig. 4. Kinetic parameters K_1 (**A**) and K_2 (**B**) of the K10, K20, and K30 powders obtained at 580 °C under 0.04 atm CO_2 at repeated sorption cycles.

3.2. Pellet development

The thermogravimetric analysis (Fig. 8A) conducted in air on both olefinic pore formers (Y and I) shows their complete degradation at 450 °C and 500 °C, respectively. Olefins degradation occurs at lower temperatures than the two sintering temperatures employed in this work (900 and 550 °C), hence the two olefins are suitable as pore formers for K_2CO_3-Li_4SiO_4 based pellet development. The smooth and sharp weight loss decay of Y and I olefins is in agreement with the ones reported in the literature for similar polyalphaolefins and indicates monodisperse oligomer distributions [38,39]. Conversely, as shown in Fig. 8A, both P and D fibres are not completely degraded in air at the lower investigated sintering temperature of 550 °C, thus resulting not suitable as pore formers using mild calcination conditions.

Fig. 8B shows the degradation in air of the selected K20 powder mixed with the largest amount (50 wt% of the total powder weight) of the more viscous olefin (I180). The K20_I50 blend present a sharp mass decay at about 350 °C obtaining a residue of 70 wt%. This weight loss (≃ 30 wt%) corresponds to the weight fraction of I180 present within the blend, hence confirming that the olefin I has been totally degraded away. In addition, the steady plateau demonstrates the stability of the final sintered pellet at the sorption/desorption temperatures (580 °C/620 °C). In fact, decomposition of Li_4SiO_4 to Li_2SiO_3 and Li_2O typically occurs at beyond 950 °C [40].

3.3. High temperature pellet sintering

Sorption/desorption tests were performed on the selected K20 powder using different concentrations of olefins I and Y (Fig. 9A-B) and sintering at 900 °C for 4 h (1 °C/min). The various pellets were labelled as K20_IXX or K20_YXX, where XX refers to the olefin percentage content on the total powder weight. Since previous results showed that 75–80 %

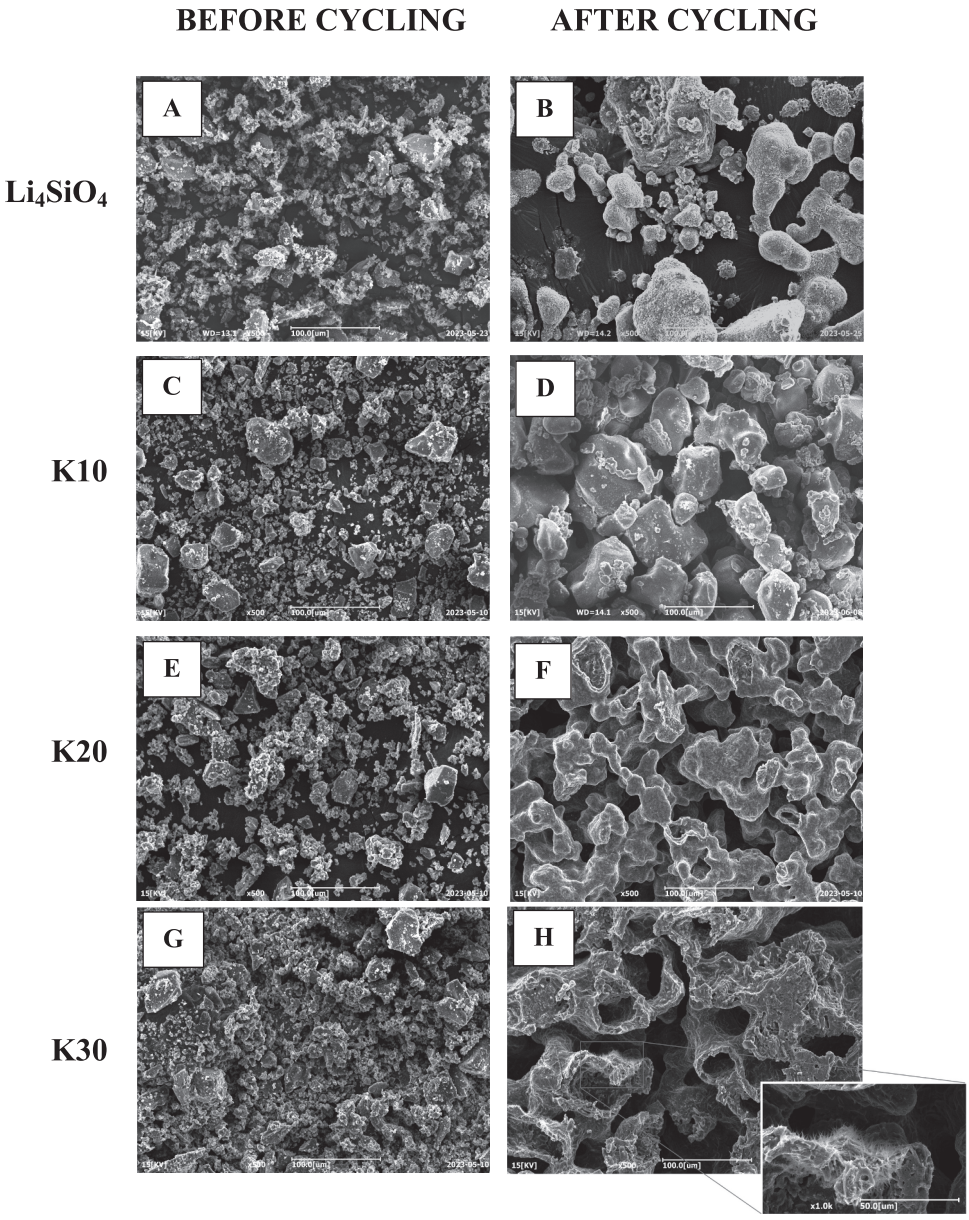

Fig. 5. SEM images of Li_4SiO_4 (**A-B**), K10 (**C-D**), K20 (**E-F**), and K30 (**G-H**) before and after eight sorption/desorption cycles.

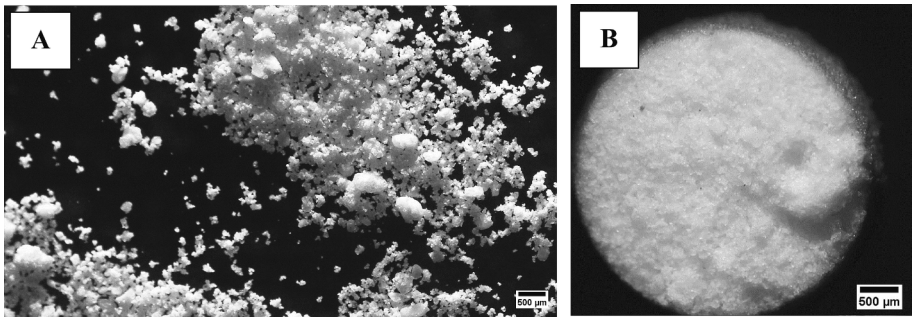

Fig. 6. Stereo-images of Li_4SiO_4 (**A**), and K30 (**B**) after eight sorption/desorption cycles.

of the maximum sorbent capacity was reached within 30 min, the tests were conducted over 30 min cycles. At the industrial level, the desorption phase starts when the CO_2 concentration at the sorbent bed outlet reaches about 20 % of the incoming CO_2 concentration. This serves as an indication that the bed has experienced breakthrough. Additional regeneration time at high temperatures did not significantly improve pellet performance. Therefore, we opted to reduce the adsorption/desorption cycle time, despite a marginal decrease in pellet capacity

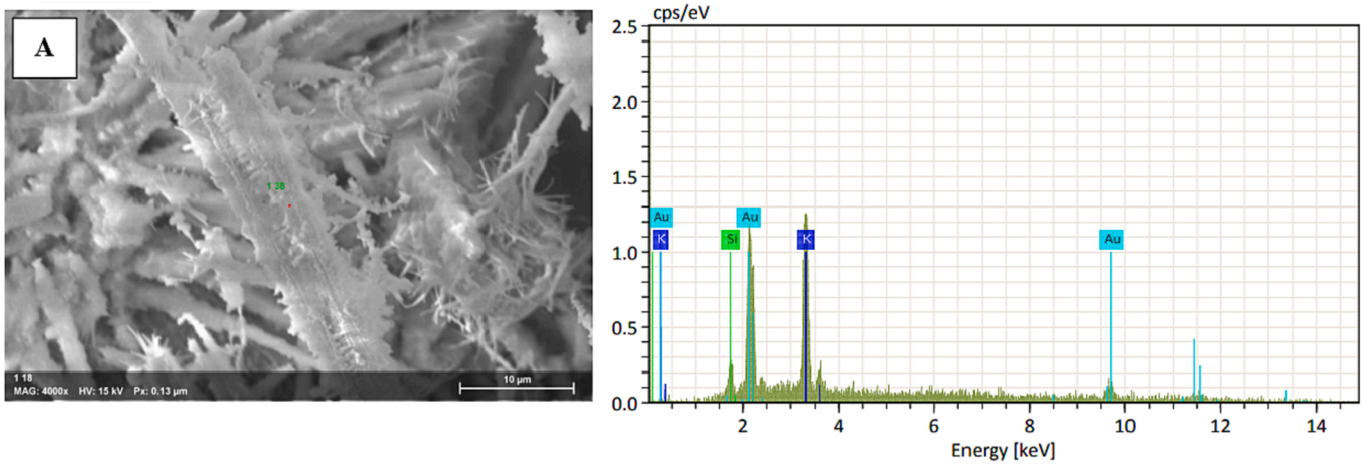

1 38

Element	At. No.	Netto	Mass [%]	Mass Norm. [%]	Atom [%]	abs. error [%] (1 sigma)
Silicon	14	380	4.25	33.85	41.61	0.35
Potassium	19	2624	8.31	66.15	58.39	0.34
Gold	79	3231	0.00	0.00	0.00	0.00
		Sum	**12.57**	**100.00**	**100.00**	

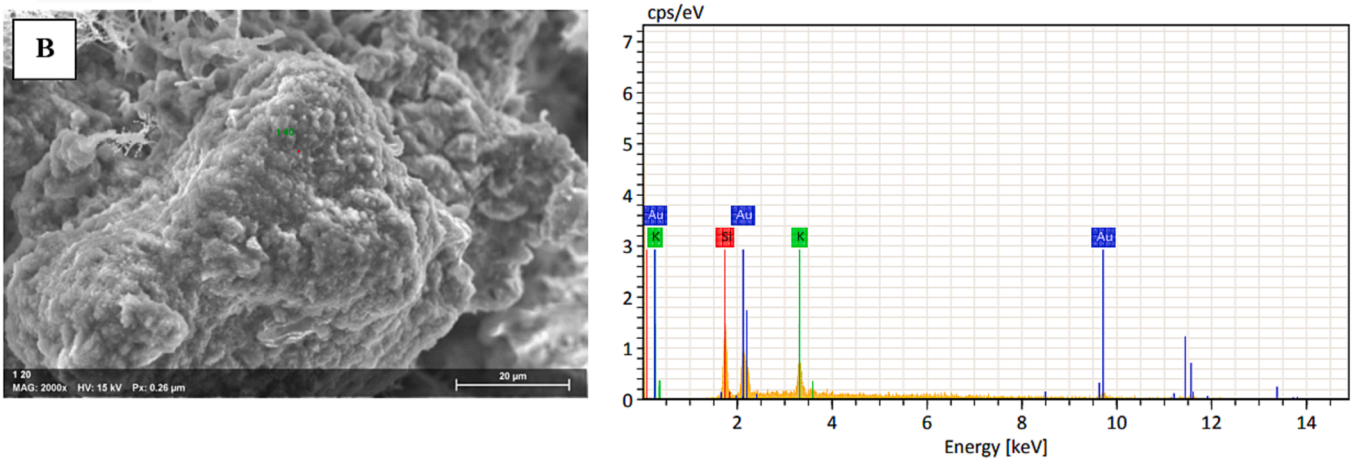

1 40

Element	At. No.	Netto	Mass [%]	Mass Norm. [%]	Atom [%]	abs. error [%] (1 sigma)
Silicon	14	1925	13.05	80.39	85.09	0.70
Potassium	19	1119	3.18	19.61	14.91	0.17
Gold	79	2318	0.00	0.00	0.00	0.00
		Sum	**16.23**	**100.00**	**100.00**	

Fig. 7. EDS microanalysis of specific areas on K30 needles (**A**) and K30 surface (**B**). The Au peak is associated with the sample surface coating with gold.

during regeneration. For the sake of clarity, to better compare the various pellets only the 8th cycles were plotted. Prior to calcination, the generated blends are easily extrudable (Fig. 10A). Following calcination, the resultant pellets become compact, white, and resistant (Fig. 10B). However, their sorption capacity remains around 1/3–1/4 of that of K20 powder regardless of the olefin type introduced and concentration.

The addition of 2 wt% of fibres (P and D) slightly increases the sorption performance of the sintered pellets due to the enhanced microporosity derived by the fibrous fillers. This is showed by the K20_I30 adsorption/desorption study reported in Fig. 11. Nonetheless, in this scenario the sorption values (60–70 $mg_{CO2}/g_{sorbent}$) are about half of the best values obtained in our previous study using layered graphite Li_4SiO_4-K_2CO_3 pellets [25]. Therefore, the use of P and D fibres cannot be considered a significant step-forward in lithium ceramic pelletisation development.

3.4. Low temperature pellet sintering

The most likely explanation for the low sorption results achieved in the previous study is that at 900 °C we are in between the two *liquidus curves* (Fig. 3). Hence, the sintering process conducted at high temperature for long time (4 h) is affected by the formation of the molten eutectic phase which tends to agglomerate the various particles reducing the porosity and surface area available for CO_2 mass transfer. To overcome this issue, the same experimental campaign carried out on the samples sintered at 900 °C was repeated using a lower sintering temperature of 550 °C for both olefins I and Y. In fact, at this temperature the eutectic phase is not yet formed while both olefins are completely degraded. Since both P and D fibres require temperatures above 600 °C

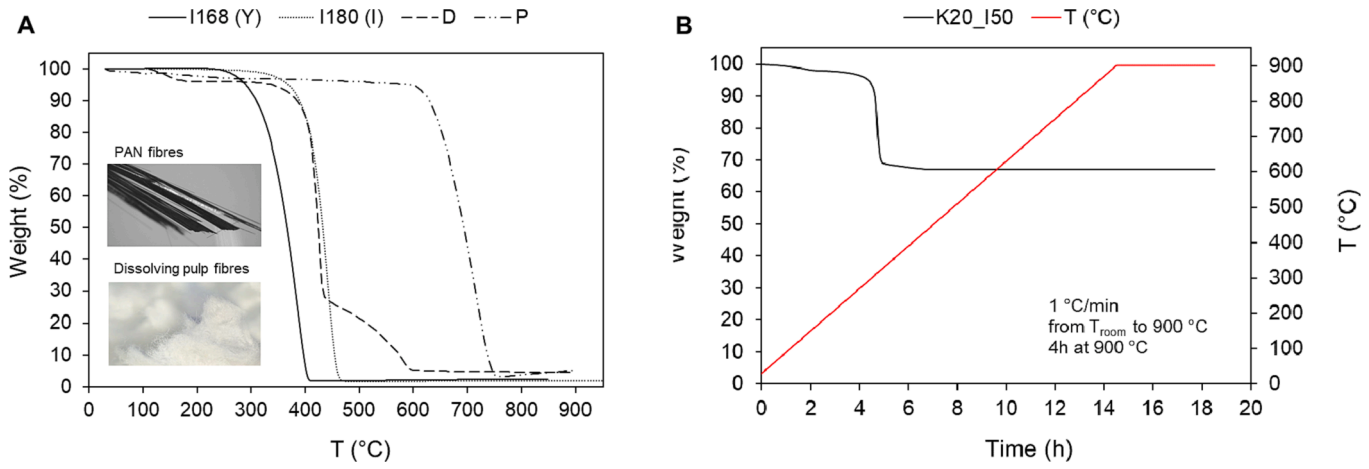

Fig. 8. TGA curves of I168 (Y) and I180 (I) polyalphaolefins, P and D fibres (**A**) and K20_I50 pellet (**B**) in air at a heating rate of 1 °C/min to 900 °C.

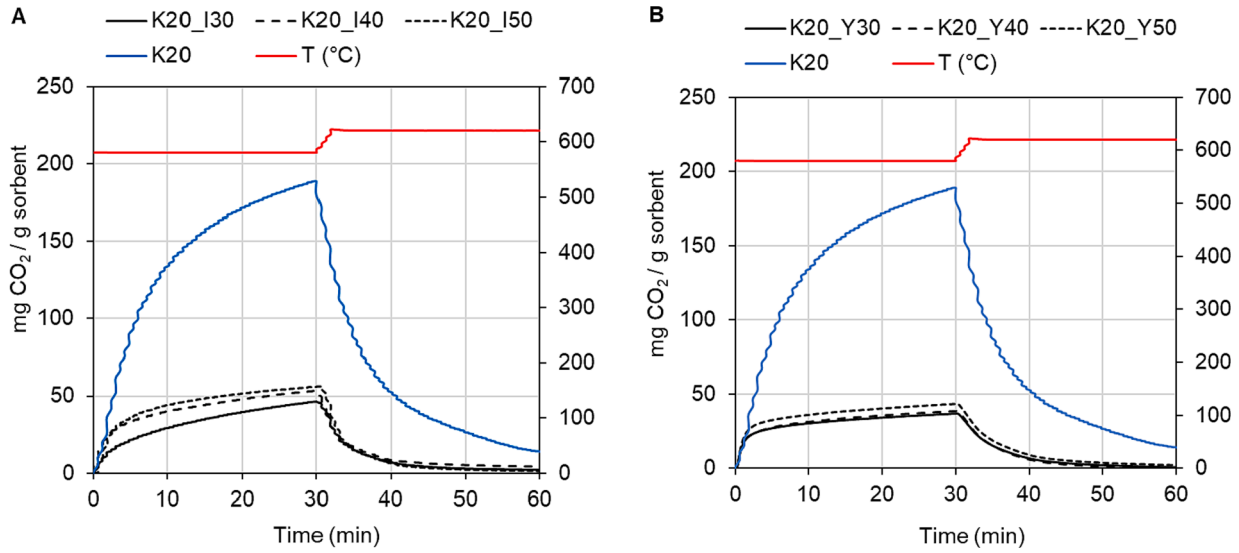

Fig. 9. 8th CO_2 sorption/desorption cycle of K20 powder (K20) versus K20 pellets (K20_IXX and K20_YXX) with 30, 40, 50 wt% of olefins I (**A**) and Y (**B**), sintered at 900 °C.

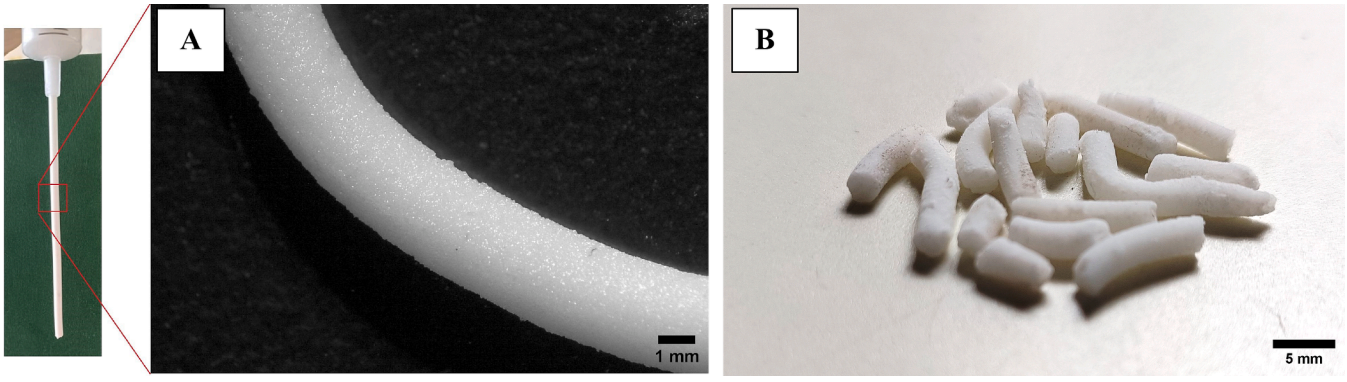

Fig. 10. K20 pellets with 30 wt% olefin I (K20_I30) before (**A**) and after (**B**) sintering at 900 °C.

to degrade completely, these were not included in the low-temperature sintering study.

For simplicity only the results obtained with the best-performing formulation (K20 with 30 wt% olefin I after low temperature sintering ("s"), labelled as K20_I30_s) were reported in Fig. 12. K20_I30_s showed a sorption capacity of 130 $mg_{CO2}/g_{sorbent}$ which is one of the highest capacities reported so far in the literature for sintered modified Li_4SiO_4 powders under low CO_2 partial pressure (below 0.1 atm). Essaki et al. 2005 reached capacities of 10–15 wt% CO_2 after 30 min adsorption in 0.04 atm of CO_2 with Li_4SiO_4-K_2CO_3-Li_2ZrO_3 sphere-type pellets

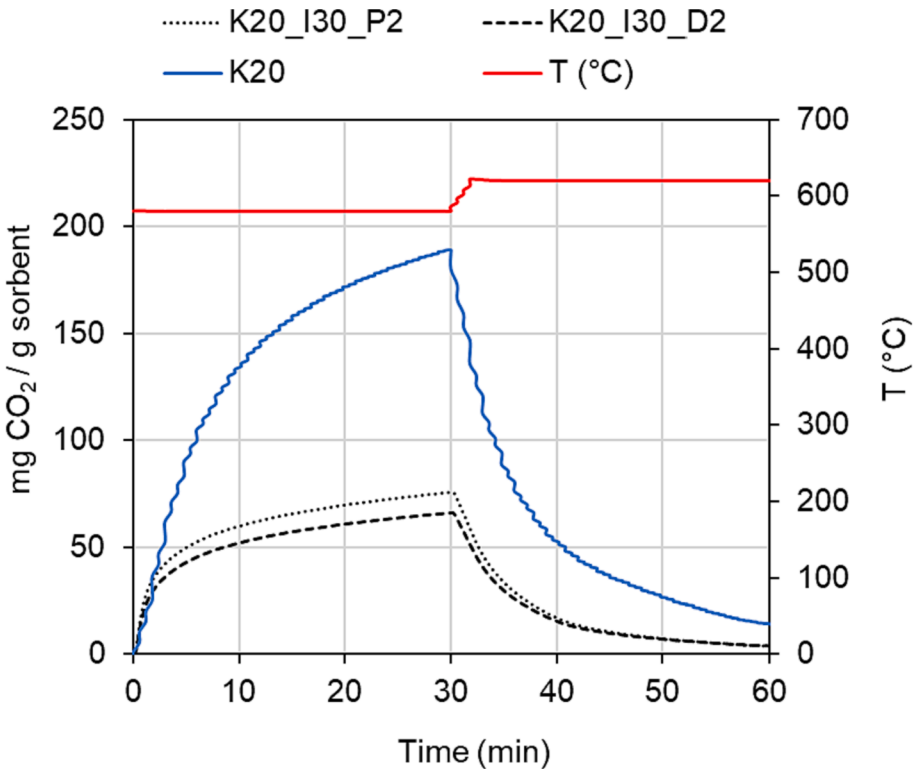

Fig. 11. 8th CO_2 sorption/desorption cycle of K20 powder (K20) versus K20 powder with 30 wt% olefins I and 2 wt% P and D fibres, sintered at 900 °C (K20_I30_P2 and K20_I30_D2, respectively).

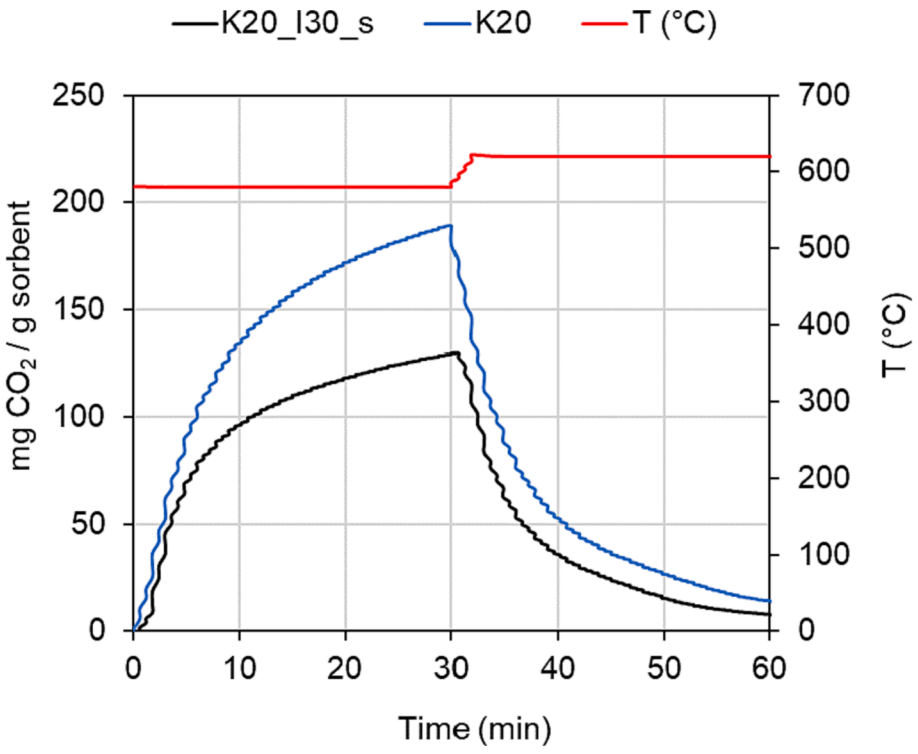

Fig. 12. 8th CO_2 sorption/desorption cycle of K20 powder (K20) versus K20 pellet sintered at 550 °C with 30 wt% olefins I, under 0.04 atm CO_2 sorption at 580 °C (30 min) and 1 atm N_2 desorption at 620 °C (30 min).

patented by Toshiba Ceramics Co. Ltd., Japan. However, the study did not evaluate sorbent cyclability over long period of time [23,24]. Seggiani et al. 2018 obtained a lower sorption capacity (110 $mg_{CO2}/g_{sorbent}$) under the same conditions with K_2CO_3-Li_4SiO_4 pellets [25]. Recently, in a similar study, Stefanelli et al. 2022 obtained sorption capacities of 100–150 $mg_{CO2}/g_{sorbent}$ after 120 min adsorption using K_2CO_3-Li_4SiO_4

based pellets which, however, required a time consuming mechanical pressurization step for pelletisation and did not allow the formation of extrudable pellet shapes [29]. All the other studies [22,26–28,30,31] which showed higher capacities (>150 $mg_{CO2}/g_{sorbent}$) were conducted on pellets tested under unrealistic conditions with CO_2 concentrations spanning from 15 up to 100 vol% which are far beyond the typical CO_2 content in hot flue gases from gas turbines. Hence, the high values obtained are largely influenced by the high CO_2 partial pressure and consequent high driving force for gas–solid mass transfer.

The improved sorption capacity achieved with the adoption of a lower sintering temperature is visible from the pellet surfaces reported in Fig. 13. K20_I30_s powders (Fig. 13A) are compacted into a rough surface with cracks and holes which facilitate CO_2 penetration through the entire inner pellet volume, whereas the surface of K20_I30 (sintered at 900 °C) results more uniform and smooth without crevices (Fig. 13B) and with segregated K_2CO_3 needles which further hinder CO_2 chemisorption (Fig. 13C).

3.5. Pellets characterization

The K20_I30_s pellet represents the best formulation developed in this study and is therefore used to obtain large cylindrical pellets (diameter = 15 mm, height = 20 mm, Fig. 14A) of suitable size to be packed into typical semi-industrial pilot-scale adsorption columns [23,24]. These large pellets resulted compact and not friable and present a uniform internal porosity which appears evenly distributed across the entire pellet inner volume (Fig. 14B). The uniform porosity is promoted by the aliphatic nature of the olefins employed as pore former that are not soluble within the K_2CO_3-Li_4SiO_4 powders thus preventing powders segregation and stratification during sintering.

The stability of the developed pellet K20_I30_s was tested over repeated 25 cycles. Different fragments from various internal and external pellet portions were used for the sorption/desorption experiments to confirm the reproducibility of the results and consequently the uniformity of sorbent properties throughout its volume. The successive sorption/desorption curves reported in Fig. 15A show a neat constant sorption capacity of about 130 $mg_{CO2}/g_{sorbent}$ (corresponding to $X_{Li4SiO4}$ of 45 %) calculated as difference between the maximum adsorption and desorption peak values.

The sorption/desorption curves slightly shift towards upper values with cycling. This behaviour was not observed in the cycling test of K20 (Fig. 2) because the sorption/desorption curves resulted from 2-hour cycles. Consequently, the regeneration reflects almost complete decarbonation, causing the curves to approach zero. On the other hand, Fig. 15A corresponds to shorter cycles of 30 min. Consequently, the regeneration process was not entirely completed. This leads to the accumulation of Li_2CO_3, Li_2SiO_3 carbonation products on the particle surface, which slightly reduces sorbent porosity. However, this negative effect is compensated by the gradual formation of the molten eutectic phase with cycling, which progressively improves sorbent capacity within the pellet volume till reaching a stable behaviour.

To validate the industrial applicability of the pellet preparation procedure, rheological tests were performed to quantify the level of mechanical energy required for the compatibilization and the extrusion of the pastes containing K20 powders and the investigated polyolefins. As shown in Fig. 16, all the samples present a strong shear-thinning behaviour typical of solid–liquid heterogeneous systems. Interestingly, the selected K20_I30 paste offers lower viscosity compared to K20_Y30 and lower viscosity at room temperature (30 °C) than 50 °C. This behaviour is in contrast if we consider that olefin I has higher viscosity than Y (1250 cSt versus 46 cSt) and the viscosity should decrease with temperature rise. These results could be explained considering that the viscosity of Y olefin is particularly low. As result, this liquid cannot stick together with particles, thus flowing out of the rheometer chamber leaving almost dried particles in contact with the rheometer plate. This outcome is supported by porosity measurements conducted on the sintered pellets which show a total porosity of 0.42 > 0.35 > 0.30 for K20_I30 (30 °C), K20_I30 (50 °C), and K20_Y30 (30 °C), respectively. At room temperature (30 °C), olefin I is absorbed more effectively by the K20 powder than Y; thus, K20_I30 is the formulation that develops the highest porosity once sintered (K20_I30_s) because more olefin remains available to form the pores. The total porosity was calculated as $(V_{pellet} - V_{powders})/V_{pellet}$, where V_{pellet} is the volume of the pellet portion determined using a pycnometer and $V_{powders}$ is the volume of the powders (K20) forming the pellets calculated as ratio between the weight and the average density of the K20 powder (≃ 2.37 g/cm^3).

The great sorption performance of K20_I30_s pellet (Fig. 12) is confirmed by its BET surface area (1.45 m^2/g) which is similar to that of starting K20 powders (2.1 m^2/g). This BET area value is one order of magnitude higher than the ones obtained using higher calcination temperatures (0.3–0.55 m^2/g) and overpass the BETs obtained in the most recent studies on lithium ceramic pellets [25,28,31].

In conclusion, K20_I30_s represents the best candidate not only in terms of sorption capacity and cyclic stability, but also for scale-up production requirements as it requires the lowest calcination temperatures and mechanical energy inputs.

4. Conclusions

A novel single-step easy method using polyalphaolefins as pore-formers was developed to produce porous K_2CO_3-Li_4SiO_4 pellets for the CO_2 capture from hot flue gases of gas turbines. The use of viscous and inert polyalphaolefins has a multiple functionality in the development of Li_4SiO_4-based pellets. At room temperature the olefin works as compatibilizer and fluidizing agent for the K_2CO_3-Li_4SiO_4 powders obtaining compact pastes which can be easily extruded to fabricate pellets of various shape and size. This method avoids time and energy consuming pelletisation technologies such as mechanical press and spheronization techniques. Furthermore, the use of low calcination temperature (550 °C), below the molten eutectic K_2CO_3-Li_2CO_3 formation, allowed the complete degradation of the olefin with consequent development of pellet porosity limiting the excessive powder sintering

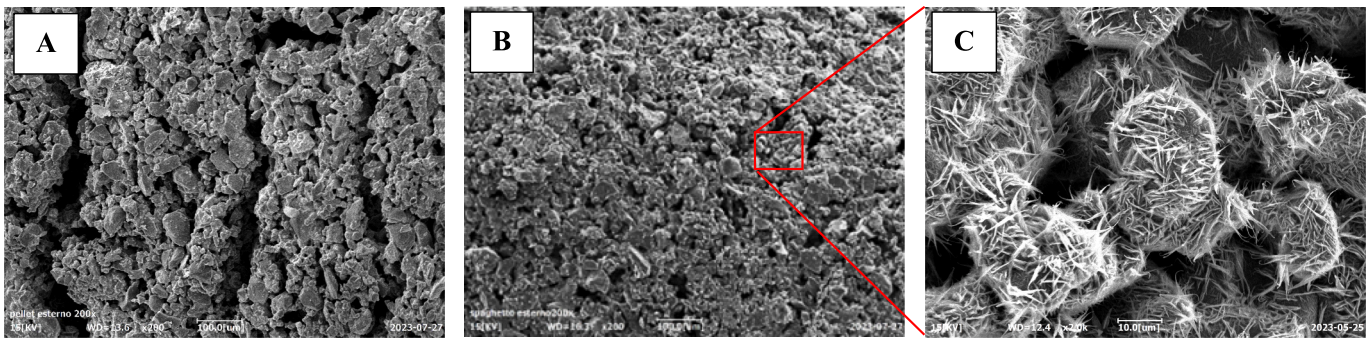

Fig. 13. SEM images of K20_I30_s (**A**) and K20_I30 (**B-C**) external surface.

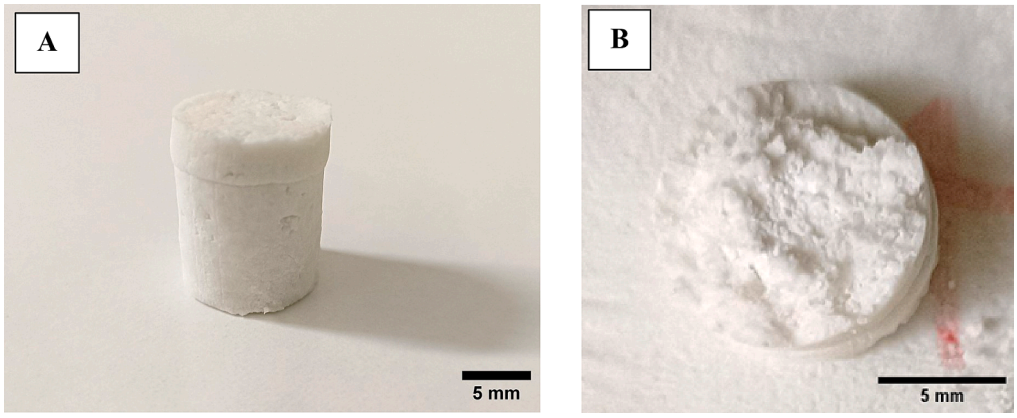

Fig. 14. K20 cylindrical pellet (**A**) and its inner volume (**B**) with 30 wt% olefin I after calcination at 550 °C (K20_I30_s).

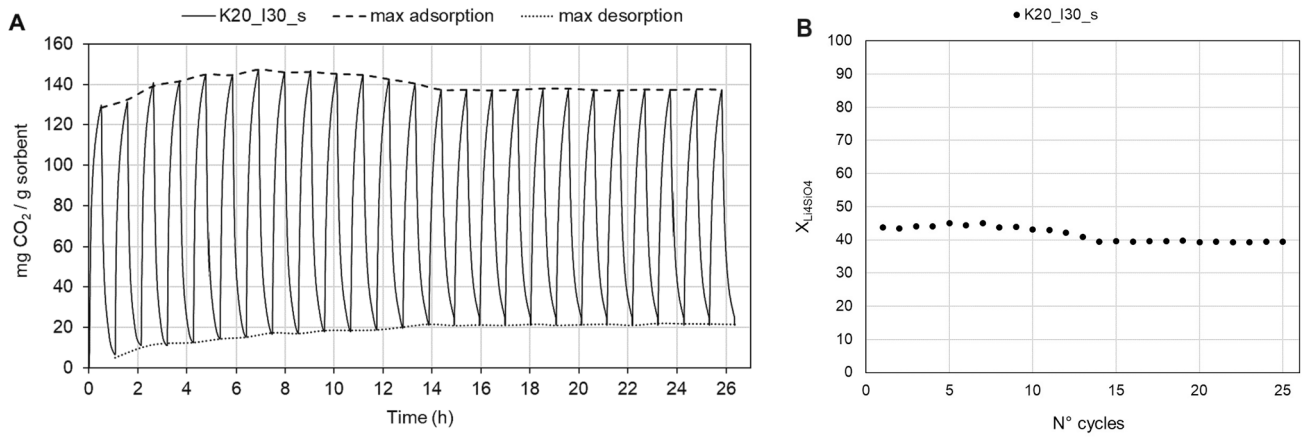

Fig. 15. Capacity (**A**) and conversion (**B**) of K20_I30_s during successive 25 CO_2 sorption/desorption cycles (0.04 atm CO_2 sorption at 580 °C (30 min) and 1 atm N_2 desorption at 620 °C (30 min)).

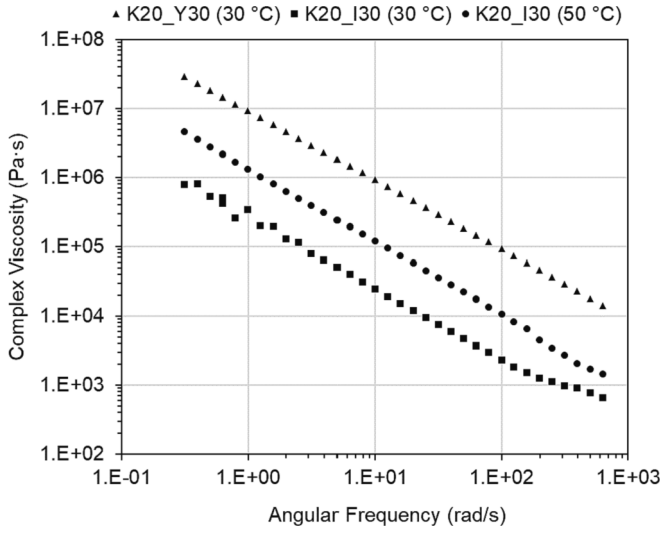

Fig. 16. Complex viscosity versus angular frequency of K20_Y30 at 30 °C and K20_I30 at 30 °C and 50 °C.

which occurs at higher temperature (900 °C). Lastly, the aliphatic nature of the olefin which is insoluble with the K_2CO_3-Li_4SiO_4 powders, actively encourages a consistent porosity preventing powders segregation, stratification, and moisture absorption during the sintering/calcination step.

The adsorption/desorption behaviour of the produced powders and pellets was evaluated by thermogravimetric analysis under 0.04 atm CO_2 at 580 °C and 1 atm N_2 at 620 °C, respectively. The sorption kinetics of the powders was fitted to the double exponential model to determine the effect of cycling and K_2CO_3 concentration on the global sorption performance. The best sorption capacity (130 $mg_{CO2}/g_{sorbent}$, $X_{Li4SiO4}$ of 45 %) was achieved using Li_4SiO_4 powder with the addition of 20 wt% of K_2CO_3 and 30 wt% high viscous olefin (1250 cSt), extruded and calcinated at 550 °C in form of cylindrical pellets (diameter = 15 mm, height = 20 mm) having a BET surface area of about 1.5 m^2/g, similar to that of starting modified powder (2.1 m^2/g).

The stability of the pellet was successfully tested over 25 repeated sorption/desorption cycles. In conclusion, the results confirmed the good sorption capacity and cyclic stability of the developed pellets which exceed those reported in similar studies, showing them suitable candidates for application in industrial fixed bed adsorption systems.

Funding

Project funded under the National Recovery and Resilience Plan (NRRP), Mission 4 Component 2 Investment 1.3 - Call for tender No. 1561 of 11.10.2022 of Ministero dell'Università e della Ricerca (MUR); funded by the European Union – NextGenerationEU. Project code PE0000021.

Credit authorship contribution statement

Damiano Rossi: Conceptualization, Data curation, Formal analysis,

Investigation, Methodology, Writing – original draft, Writing – review & editing, Validation, Visualization. **Irene Anguillesi:** Formal analysis, Investigation, Methodology. **Umberto Desideri:** Resources, Writing – review & editing. **Maurizia Seggiani:** Methodology, Resources, Supervision, Writing – review & editing.

Declaration of competing interest

The authors declare that they have no known competing financial interests or personal relationships that could have appeared to influence the work reported in this paper.

Data availability

Data will be made available on request.

Acknowledgements

The authors would like to acknowledge Ineos Oligomers Ltd (US) for providing Durasyn® polyalphaolefin samples, MAE Spa (Italy) for providing natural and synthetic fibre samples, and CISUP (Centre for Instrument Sharing of the University of Pisa) for the access to FEI Quanta 450 FEG Environmental Scanning Electron Microscope (ESEM).

Project funded under the National Recovery and Resilience Plan (NRRP), Mission 4 Component 2 Investment 1.3 - Call for tender No. 1561 of 11.10.2022 of Ministero dell'Università e della Ricerca (MUR); funded by the European Union – NextGenerationEU. Project code PE0000021.

References

[1] IEA2023 Available online: https://www.iea.org/reports/global-energy-review-co2-emissions-in-2021-2.
[2] R. Soundararajan, T. Gundersen, Coal Based Power Plants Using Oxy-Combustion for CO2 Capture: Pressurized Coal Combustion to Reduce Capture Penalty, Appl. Therm. Eng. 61 (2013) 115–122, https://doi.org/10.1016/j.applthermaleng.2013.04.010.
[3] D. Panda, V. Kulkarni, S.K. Singh, Evaluation of Amine-Based Solid Adsorbents for Direct Air Capture: A Critical Review, React. Chem. Eng. 8 (2022) 10–40, https://doi.org/10.1039/d2re00211f.
[4] A. Jha, V. Ravuru, M. Yadav, S.D.A. Mandal, A Critical Analysis of CO2 Capture Technologies, Hydrocarb. Process. (2021) 59–65.
[5] González-Varela, D.; Hernández-Fontes, C.; Wang, N.; Pfeiffer, H. State of the Art and Perspectives of the CO2 Chemisorption in Ceramics with Its Simultaneous or Subsequent Chemical Transformation. Carbon Capture Sci. Technol. **2023**, *7*, doi: 10.1016/j.ccst.2023.100101.
[6] S. Kumar, R. Srivastava, J. Koh, Utilization of Zeolites as CO2capturing Agents: Advances and Future Perspectives, J. CO2 Util. 41 (2020) 101251, https://doi.org/10.1016/j.jcou.2020.101251.
[7] A.A. Abd, M.R. Othman, J. Kim, A Review on Application of Activated Carbons for Carbon Dioxide Capture: Present Performance, Preparation, and Surface Modification for Further Improvement, Environ. Sci. Pollut. Res. 28 (2021) 43329–43364, https://doi.org/10.1007/s11356-021-15121-9.
[8] S. Castro-Pardo, S. Bhattacharyya, R.M. Yadav, A.P. de Carvalho Teixeira, M. A. Campos Mata, T. Prasankumar, M.A. Kabbani, M.G. Kibria, T. Xu, S. Roy, et al., A Comprehensive Overview of Carbon Dioxide Capture: From Materials, Methods to Industrial Status, Mater. Today 60 (2022) 227–270, https://doi.org/10.1016/j.mattod.2022.08.018.
[9] Y. Hu, W. Liu, Y. Yang, M. Qu, H. Li, CO2 Capture by Li4SiO4 Sorbents and Their Applications: Current Developments and New Trends, Chem. Eng. J. 359 (2019) 604–625, https://doi.org/10.1016/j.cej.2018.11.128.
[10] Z. Qiao, Z. Wang, C. Zhang, S. Yuan, Y. Zhu, J. Wang, Analysis of CO2 Sorption/Desorption Kinetic Behaviors and Reaction Mechanisms on Li4SiO4, AIChE J. 59 (2012) 215–228, https://doi.org/10.1002/aic.13861.
[11] J. Ortiz-Landeros, T.L. Ávalos-Rendón, C. Gómez-Yáñez, H. Pfeiffer, Analysis and Perspectives Concerning CO2 Chemisorption on Lithium Ceramics Using Thermal Analysis, J. Therm. Anal. Calorim. 108 (2012) 647–655, https://doi.org/10.1007/s10973-011-2063-y.
[12] J.I. Ida, Y.S. Lin, Mechanism of High-Temperature CO2 Sorption on Lithium Zirconate, Environ. Sci. Technol. 37 (2003) 1999–2004, https://doi.org/10.1021/es0259032.
[13] K. Wang, Z. Zhou, P. Zhao, Z. Yin, Z. Su, J. Sun, Molten Sodium-Fluoride-Promoted High-Performance Li4SiO4-Based CO2 Sorbents at Low CO2 Concentrations, Appl. Energy 204 (2017) 403–412, https://doi.org/10.1016/j.apenergy.2017.07.072.
[14] Y. Tong, S. Chen, X. Huang, Y. He, J. Chen, C. Qin, CO2 Capture by Li4SiO4 Sorbents: From Fundamentals to Applications, Sep. Purif. Technol. 301 (2022) 121977, https://doi.org/10.1016/j.seppur.2022.121977.
[15] X. Yang, W. Liu, J. Sun, Y. Hu, W. Wang, H. Chen, Y. Zhang, X. Li, M. Xu, Alkali-Doped Lithium Orthosilicate Sorbents for Carbon Dioxide Capture, ChemSusChem 9 (2016) 2480–2487, https://doi.org/10.1002/cssc.201600737.
[16] Kato Masahiro, N.K.; Nakagawa, Y.T.; Ohashi, K.S.; Essaki, Y.K. Carbon Dioxide Gas Absorbent Containing Lithium Silicate 2002, *US Patent*.
[17] M. Kato, S. Yoshikawa, K. Nakagawa, Carbon Dioxide Absorption by Lithium Orthosilicate in a Wide Range of Temperature and Carbon Dioxide Concentrations, J. Mater. Sci. Lett. 21 (2002) 485–487, https://doi.org/10.1023/A:1015338808533.
[18] M. Seggiani, M. Puccini, S. Vitolo, High-Temperature and Low Concentration CO2 Sorption on Li4SiO4 Based Sorbents: Study of the Used Silica and Doping Method Effects, Int. J. Greenh. Gas Control 5 (2011) 741–748, https://doi.org/10.1016/j.ijggc.2011.03.003.
[19] M. Seggiani, M. Puccini, S. Vitolo, Alkali Promoted Lithium Orthosilicate for CO2 Capture at High Temperature and Low Concentration, Int. J. Greenh. Gas Control 17 (2013) 25–31, https://doi.org/10.1016/j.ijggc.2013.04.009.
[20] S. Zhang, Q. Zhang, H. Wang, Y. Ni, Z. Zhu, Absorption Behaviors Study on Doped Li4SiO4 under a Humidified Atmosphere with Low CO2 Concentration, Int. J. Hydrogen Energy 39 (2014) 17913–17920, https://doi.org/10.1016/j.ijhydene.2014.07.011.
[21] Z. Zhou, K. Wang, Z. Yin, P. Zhao, Z. Su, J. Sun, Molten K2CO3-Promoted High-Performance Li4SiO4 Sorbents at Low CO2 Concentrations, Thermochim. Acta 655 (2017) 284–291, https://doi.org/10.1016/j.tca.2017.07.014.
[22] M. Kato, K. Essaki, S. Yoshikawa, K. Nakagawa, H. Uemotoþ, Reproducibility of CO2 Absorption and Emission for Cylindrical Pellet Type Lithium Orthosilicate, J. Ceram. Soc. Japan 1340 (2004) 1338–1340.
[23] K. Essaki, M. Kato, H. Uemoto, Influence of Temperature and CO2 Concentration on the CO2 Absorption Properties of Lithium Silicate Pellets, J. Mater. Sci. 40 (2005) 5017–5019, https://doi.org/10.1007/s10853-005-1812-3.
[24] K. Essaki, M. Kato, K. Nakagawa, CO2 Removal at High Temperature Using Packed Bed of Lithium Silicate Pellets, J. Ceram. Soc. Japan 114 (2006) 739–742, https://doi.org/10.2109/jcersj.114.739.
[25] M. Seggiani, E. Stefanelli, M. Puccini, S. Vitolo, CO2 Sorption/Desorption Performance Study on K2CO3-Doped LI4SIO4-Based Pellets, Chem. Eng. J. 339 (2018) 51–60, https://doi.org/10.1016/j.cej.2018.01.117.
[26] Y. Yang, W. Liu, Y. Hu, J. Sun, X. Tong, Q. Chen, Q. Li, One-Step Synthesis of Porous Li4SiO4-Based Adsorbent Pellets via Graphite Moulding Method for Cyclic CO2 Capture, Chem. Eng. J. 353 (2018) 92–99, https://doi.org/10.1016/j.cej.2018.07.044.
[27] Y. Hu, M. Qu, H. Li, Y. Yang, J. Yang, W. Qu, W. Liu, Porous Extruded-Spheronized Li4SiO4 Pellets for Cyclic CO2 Capture, Fuel 236 (2019) 1043–1049, https://doi.org/10.1016/j.fuel.2018.09.072.
[28] L. Ma, C. Qin, S. Pi, H. Cui, Fabrication of Efficient and Stable Li4SiO4-Based Sorbent Pellets via Extrusion-Spheronization for Cyclic CO2 Capture, Chem. Eng. J. 379 (2020) 122385, https://doi.org/10.1016/j.cej.2019.122385.
[29] E. Stefanelli, S. Vitolo, M. Puccini, Single-Step Fabrication of Templated Li4SiO4-Based Pellets for CO2capture at High Temperature, J. Environ. Chem. Eng. 10 (2022) 108389, https://doi.org/10.1016/j.jece.2022.108389.
[30] Stefanelli, E.; Vitolo, S.; Frano, R. Lo; Pesetti, A.; Aquaro, D.; Puccini, M. Li4SiO4 Breeder Pebbles Fabrication by a Sol-Gel Supported Drip Casting Method. Fusion Eng. Des. **2022**, *175*, 113014, doi:10.1016/j.fusengdes.2022.113014.
[31] R. Fu, G. Yu, J. Cheng, Y. Hu, S. Yan, One-Step Synthesis of Porous Li4SiO4 Pellets by Polyvinyl Alcohol (PVA) Method for CO2 Capture, Fuel 331 (2023) 1–8, https://doi.org/10.1016/j.fuel.2022.125873.
[32] L. Ma, S. Chen, C. Qin, S. Chen, W. Yuan, X. Zhou, J. Ran, Understanding the Effect of H2S on the Capture of CO2 Using K-Doped Li4SiO4 Sorbent, Fuel 283 (2021) 119364, https://doi.org/10.1016/j.fuel.2020.119364.
[33] E. Stefanelli, M. Puccini, S. Vitolo, M. Seggiani, CO2 Sorption Kinetic Study and Modeling on Doped-Li4SiO4 under Different Temperatures and CO2 Partial Pressures, Chem. Eng. J. 379 (2020) 122307, https://doi.org/10.1016/j.cej.2019.122307.
[34] M.J. Venegas, E. Fregoso-Israel, R. Escamilla, H. Pfeiffer, Kinetic and Reaction Mechanism of CO2 Sorption on Li 4SiO4: Study of the Particle Size Effect, Ind. Eng. Chem. Res. 46 (2007) 2407–2412, https://doi.org/10.1021/ie061259e.
[35] H. Pfeiffer, P. Bosch, S. Bulbulian, Synthesis of Lithium Silicates, J. Nucl. Mater. 257 (1998) 309–317, https://doi.org/10.1016/S0022-3115(98)00449-8.
[36] FactSageTM, FACT Salt Database, (2007). Available online: www.factsage.cn/fact/documentation.
[37] M.J. Venegas, E. Fregoso-Israel, R. Escamilla, H. Pfeiffer, Kinetic and Reaction Mechanism of CO2 Sorption on Li4SiO4: Study of the Particle Size Effect, Ind. Eng. Chem. Res. 46 (2007) 2407–2412, https://doi.org/10.1021/ie061259e.
[38] Y. Ma, J. Xu, X. Zeng, H. Jiang, J. Li, Preparation and Performance Evaluation of MPAO8 Using Olefin from Coal as Raw Material, Ind. Lubr. Tribol. 69 (2017) 678–682, https://doi.org/10.1108/ILT-03-2016-0049.
[39] Q. Yu, C. Zhang, R. Dong, Y. Shi, Y. Wang, Y. Bai, J. Zhang, M. Cai, F. Zhou, W. Liu, Physicochemical and Tribological Properties of Gemini-Type Halogen-Free Dicationic Ionic Liquids, Friction 9 (2021) 344–355, https://doi.org/10.1007/s40544-019-0348-5.
[40] D. Cruz, S. Bulbulian, E. Lima, H. Pfeiffer, Kinetic Analysis of the Thermal Stability of Lithium Silicates (Li4SiO4 and Li2SiO3), J. Solid State Chem. 179 (2006) 909–916, https://doi.org/10.1016/j.jssc.2005.12.020.